Bioconjugate Chemistry

Article

Cite This: Bioconjugate Chem. 2018, 29, 2763−2775

pubs.acs.org/bc

Development and Characterization of Peptide Ligands of Immunoglobulin G Fc Region

Nika Kruljec,[†,‡] Peter Molek,[†] Vesna Hodnik,[§,∥] Gregor Anderluh,[∥] and Tomaž Bratkovič*[,†]

[†]University of Ljubljana, Faculty of Pharmacy, Department of Pharmaceutical Biology, SI-1000 Ljubljana, Slovenia

[‡]University of Ljubljana, Faculty of Medicine, Graduate School of Biomedicine, Ljubljana, SI-1000 Slovenia

[§]University of Ljubljana, Biotechnical Faculty, Department of Biology, SI-1000 Ljubljana, Slovenia

[∥]National Institute of Chemistry, Department of Molecular Biology and Nanobiotechnology, SI-1000 Ljubljana, Slovenia

Supporting Information

ABSTRACT: Affinity chromatography based on bacterial immunoglobulin (Ig)-binding proteins represents the cornerstone of therapeutic antibody downstream processing. However, there is a pressing need for more robust affinity ligands that would withstand the harsh column sanitization conditions, while still displaying high selectivity for antibodies. Here, we report the development of linear peptide IgG ligands, identified from combinatorial phage-display library screens. The lead peptide was shown to compete with staphylococcal protein A for the IgG Fc region. Trimming analysis and alanine scanning revealed the minimal structural requirements of the peptide for Fc binding, and the minimized peptide GSYWYQVWF recognized all human IgG subtypes. Mutation of glutamine located at the nonessential position 6 to aspartate led to the optimized peptide GSYWYDVWF with 18-fold higher affinity (K_D app. 0.6 μM) compared to the parent peptide. When coupled to paramagnetic beads or a chromatographic matrix, the optimized ligand was shown to selectively enrich antibodies from complex protein mixtures.

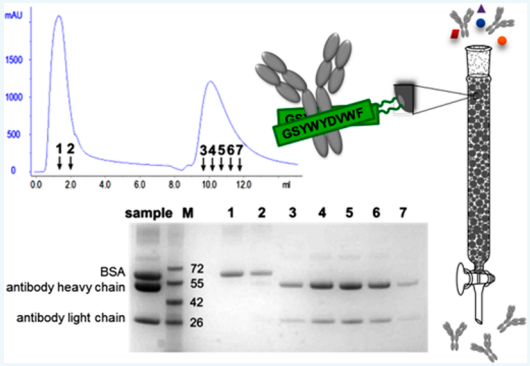

INTRODUCTION

In the past three decades, the number of therapeutic and diagnostic antibodies has been growing at an astonishing rate.[1,2] Antibodies have established themselves as the leading biopharmaceutical modality due to their high specificity and affinity, predictable pharmacokinetics, and favorable toxicological profiles. Substantial progress in upstream processing of recombinant therapeutic antibodies has shifted the production bottleneck to downstream processing steps. Accordingly, downstream processing was estimated to contribute a significant percentage (as much as 80%) to total antibody production cost.[3] Thus, considerable efforts have been invested into development of improved purification schemes and cost-effective innovative separation technologies.[4−6]

The biopharmaceutical industry adopted affinity chromatography as the initial capture step in the antibody purification process. Because of high specificity, the most commonly used affinity matrices are based on bacterial immunoglobulin (Ig)-binding proteins such as staphylococcal protein A (SpA) and streptococcal protein G (SpG).[7] However, such affinity ligands suffer from several drawbacks.[8] They are produced by recombinant DNA technology, which is reflected in expensive affinity columns. Moreover, high affinity for antibodies necessitates harsh elution conditions that can negatively impact structure, and hence the function and immunogenicity of recombinant antibodies.[9] Furthermore, ligand instability (susceptibility to column sanitization and elution conditions, and especially proteases) translates to limited column lifetime and requires extensive efforts to eliminate immunogenic leached ligands from the final product.[10]

Among alternative antibody ligands,[11] short peptides are an especially attractive option for chromatographic purposes. Provided they are structurally simple (relatively short and linear), they can be affordably synthesized even on a large scale. They possess favorable toxicity and immunogenicity profiles, and their stability is relatively high compared to larger proteins that rely on a complex folding pattern for the formation of binding sites. Furthermore, peptide ligands typically bind to target proteins with only moderate affinity, suggesting that mild conditions should be sufficient for breaking the interaction with immunoglobulins. Leaching of peptides from affinity matrices can be minimized by engineering protease-resistant features in peptides, such as incorporation of non-natural amino acids or replacement of the peptide backbone with a nonpeptide framework.

Received: June 7, 2018
Revised: July 12, 2018
Published: July 19, 2018

DOI: 10.1021/acs.bioconjchem.8b00395
Bioconjugate Chem. 2018, 29, 2763−2775

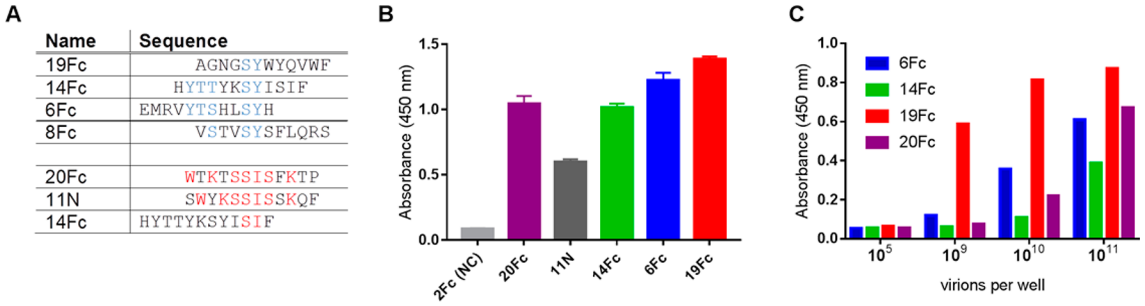

Figure 1. Characterization of hits identified in library screening. (A) Alignment of amino acid sequences of hFc binding peptides. Two distinct consensus motifs are color-coded in blue and red. (B) Comparative affinities for hFc of representative phage clones displaying peptides containing both identified amino acid motifs as assessed by phage ELISA. Phage clone 2Fc (Figure S2A) was used as the negative control (NC). Each clone was contacted with hFc-coated wells at 10^{10} virions/well. The experiment was performed in triplicate. (C) Concentration-dependent binding to hFc of clones displaying different peptides in a monovalent format (single peptide copy per virion) as evaluated by phage ELISA.

Several peptide affinity ligands of immunoglobulins have been reported.[11] One of them (D-PAM, a dendrimer protein A mimetic, composed of four copies of D-amino acid tripeptide RTY[12]) has made it to the market (Kaptiv-GY; Interchim, Montluçon, France). However, with the exception of the hexapeptide ligand HWRGWV identified by synthetic peptide library screening,[13−15] the rationally designed SpA mimetic octapeptide FYWHCLDE,[16] and Fcγ receptor-derived octapeptides NKFRGKYK and NARKFYKG,[17] affinity peptides typically relied on cyclization[18−20] for lowering the entropic barrier upon binding of otherwise flexible peptides or on linking several copies into dendrimers,[12,21,22] augmenting avidity effects in order to achieve sufficient affinities required for antibody affinity purification. The requirement for such peptide modifications complicates synthetic procedures and can lead to diminished production yield. While peptide phage display libraries have been used before to screen for IgG binding peptides,[23−26] this is the first report of development of high-affinity short *linear* peptides selectively binding the Fc region of immunoglobulin G for use in diverse applications such as antibody affinity chromatography, antibody pull-down, and uniform antibody immobilization. The lead peptide was identified from a large phage-display library of random dodecapeptides in tailored affinity screens against the Fc region of human IgG and was shown to compete with SpA for Fc binding. In trimming and alanine scanning analyses conducted in the course of deducing the minimal structural requirements for antibody binding, we conveniently used peptides displayed on a dedicated phage vector, thus avoiding time-consuming and costly customized peptide synthesis. The minimized nonapeptide ligand recognized all subclasses of human IgGs as well as all tested mammalian IgGs. Amino acid at a nonessential position was mutated to charged residues, resulting in an improved peptide ligand with ∼18-fold higher affinity. Functional pull-down assays were performed to demonstrate the synthetic peptides' capacity to selectively enrich IgGs from human serum, and a prototype affinity column based on the optimized peptide ligand was prepared and characterized with respect to selectivity and dynamic binding capacity.

RESULTS AND DISCUSSION

Selection of Fc Binders from Phage Peptide Libraries. We have screened three commercially available phage display random peptide libraries (linear hepta- and dodecapeptides, and cyclic nonapeptides of the CX_7C type) with the goal of identifying structurally simple ligands for the IgG Fc fragment. A three-cycle biopanning procedure in solution was tailored to incrementally increase stringency during selection: the amount of the target was gradually reduced throughout the selections, contact time of the phage library with the target was reduced, and the number of washing steps was increased. Moreover, competitive elution in the second and third selection rounds was introduced to guide selection toward selective human Fc binders, while continuous presence of bovine serum albumin (BSA) in binding and washing buffers ensured that no albumin binders were enriched. To further improve the specificity of biopanning, negative selection steps against streptavidin beads (the matrix used to capture phage−Fc complexes) were introduced before the second and the third selection rounds. In addition, isolation of streptavidin binders was prevented by adding biotin to the buffer during the last washing step.

We monitored the enrichment of Fc-binding phages throughout the affinity selection process by calculating the proportion of eluted phages after individual selection rounds relative to the input phage numbers. We observed a marked increase in percentage of eluted phages after the third selection round only in the biopanning experiment with the PhD-12 library (Figure S1A); no significant enrichment was seen with PhD-7 and PhD-C7C libraries (data not shown). The reasons for unproductive pannings with the PhD-7 and PhD-C7C libraries may lie in suboptimal length and conformational constraints of the displayed peptides, respectively.

Amplified pools of eluted phages after each of the three selection rounds were subjected to phage ELISA (Figure S1B). An incremental increase in signals from first through third selection round phages was observed, which further confirms selective enrichment of Fc-binders. Importantly, no interaction of phage pools with either streptavidin (capturing component) or BSA (blocking agent) was observed.

After the last round of biopanning, 40 individual clones were randomly picked (20 clones resulting from screens employing competitive elution with human Fc fragment (denoted 1Fc to 20Fc) and 20 clones from screens employing nonspecific elution (denoted 1N to 20N)) and amplified in host bacterial cultures. Their interaction with human Fc (hFc) was evaluated with qualitative phage ELISA (Figure S2). According to the arbitrary criteria of absorbance being higher than 0.5 and signal-to-background ratio (i.e., binding to hFc- vs BSA-coated (blank) wells) ≥ 4, a total of 24 phage clones (60%) showed specific binding to the human Fc fragment. DNA extracted from positive clones was sequenced to deduce the primary

DOI: 10.1021/acs.bioconjchem.8b00395
Bioconjugate Chem. 2018, 29, 2763−2775

structures of displayed peptides. Altogether, six Fc-binders were identified and classified into two groups according to the amino acid consensus motifs (color-coded in Figure 1A); peptide 14Fc contained elements of both consensus motifs. In general, peptide ligands were enriched in hydroxyl-group-containing and aromatic residues, and a previously identified Fc-binding motif SSI[23,26] was observed in one of the peptide consensus groups.

Characterization of Hits Identified in Library Screening. Affinities of representative clones for the human Fc fragment were compared in phage ELISA assay using equal amounts of phages (10^{10} virions/well). Four phage clones (6Fc, 14Fc, 19Fc, and 20Fc) produced strong signals, while 11N bound the target only moderately (Figure 1B). On the M13KE phage, the parent of PhD libraries, the peptides are displayed in up to five copies. To avoid avidity effects, we displayed peptides 6Fc, 14Fc, 19Fc, and 20Fc on virions in the monovalent format (less than one copy per virion on average) using a phagemid-based system and reanalyzed their relative affinities to hFc. In the monovalent format, significant differences were seen in concentration-dependent phage binding to hFc (Figure 1C). Because of its strong binding even at very low concentrations (10^9 virions/well), clone 19Fc was chosen for further characterization. Another reason for choosing 19Fc as the lead peptide was the lack of a previously identified Fc-binding motif as opposed to the SSI tripeptide in peptide 20Fc.

In a modified fluorescence-linked immunosorbent assay (FLISA), fluorescein-labeled 19Fc phage competed with immunoglobulin-binding staphylococcal protein A (SpA) for hFc binding in a concentration-dependent manner (Figure 2). This indicates that the 19Fc peptide's binding site at least partially overlaps with that of SpA (located at the CH_2 and CH_3 domain interface[27]).

Minimization of 19Fc Parent Peptide. In an attempt to identify the minimal structure and critical residues of the lead peptide required for Fc binding, a series of N- and C-terminally trimmed peptides based on the amino acid sequence of 19Fc was designed (Figure 3) and displayed on the M13KBE phage, a variant of the M13KE vector (Supporting Information Methods and Figure S3). Phage clones were subjected to phage ELISA, and the affinities of individual peptide variants were compared to that of the parent peptide 19Fc to identify the minimal motif required for hFc binding.[28] It should be noted that due to avidity effects inherent to pentavalent display, the assay is likely to be sensitive only to large differences in peptide affinities. When the C-terminal Phe12 was removed, the peptide (19Fc-1) completely lost the ability to bind hFc. The same was observed for peptide variants lacking six N-terminal residues (i.e., up to including Tyr6). On the other hand, amino-terminal trimming up to including Ser5 was well tolerated in terms of Fc binding affinity. However, the 19Fc-6 variant lacking Ser5 displayed higher nonspecific binding, likely because Ser5 is the only hydrophilic residue (apart from Gln9) in the otherwise highly hydrophobic peptide. Moreover, the serine residue was part of the initially identified consensus sequence (Figure 1A). Therefore, we decided to keep the Ser5 in the minimized peptide ligand GSYWYQVWF, hereafter termed min19Fc.

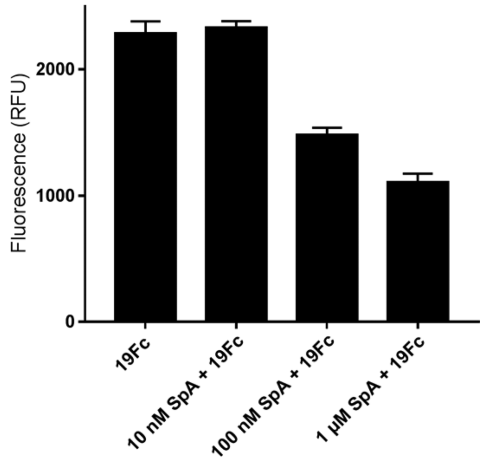

Figure 2. Competitive binding of fluorescein-labeled 19Fc phage clone (1.2×10^{10} virions/well) and staphylococcal protein A for immobilized hFc. Signals from blank (BSA-coated) wells were subtracted from fluorescence values of paired test wells. The experiment was performed in triplicate. RFU, relative fluorescence units.

Reactivity of Minimized Peptide minFc19 with Different IgGs. The Fc-binding activity of the min19Fc-displaying phage was evaluated by phage ELISA using different therapeutic monoclonal antibodies and human IgG subclasses as targets. Due to differences in formulation of antibodies that might affect target adsorption to microtiter plate wells, the assay is considered qualitative. Phage clone min19Fc bound to all human IgG subclasses as well as all tested therapeutic monoclonal antibodies (Figure 4A) but displayed no significant binding to any of the negative controls (BSA, avidin, and streptavidin), suggesting specificity of min19Fc for the Fc fragment of IgGs.

Peptide min19Fc is highly hydrophobic. To augment the solubility of its synthetic biotinylated version b-min19Fc, we added a hydrophilic linker GGGSKKK(ε-biotin)-$CONH_2$ to its C-terminus. Binding activity of b-min19Fc to IgGs of different animal species (mouse, rabbit, donkey, and goat) was qualitatively assessed; the biotinylated peptide was complexed to streptavidin (SA) and adsorbed onto microtiter plate wells. Coated wells were contacted with mouse, donkey, rabbit, and goat IgG-horseradish peroxidase (HRP) conjugates, and binding was detected with a peroxidase chromogenic substrate. In addition to human antibodies, min19Fc exhibited binding to all tested nonhuman IgGs (Figure 4B).

Characterization of the Interaction between the min19Fc Peptide and Human IgG Fc Fragment Using Surface Plasmon Resonance. The interaction of the human Fc fragment with synthetic peptide b-min19Fc was analyzed by surface plasmon resonance using the Biacore X100. Biotinylated peptide b-min19Fc was immobilized to a streptavidin-coupled chip, and the hFc fragment was passed over the surface. We used the single-cycle kinetics approach, where the analyte is successively injected in increasing concentrations without intermediate surface regeneration between individual injections.[29] In Figure 5, a single sensorgram recorded upon successive injections of human IgG Fc fragment at five progressively increasing concentrations is depicted (overlaid sensorgrams from independent recordings are shown in Figure S4). A near perfect fit of the binding curves with the bivalent analyte model (BiaEvaluation software) was obtained, suggesting that two peptide ligands bind the homodimeric Fc fragment. No binding was detected when BSA (1 μM) was injected over the sensor surface (not shown), indicating

DOI: 10.1021/acs.bioconjchem.8b00395
Bioconjugate Chem. 2018, 29, 2763−2775

Name	Sequence
19Fc	AGNGSYWYQVWF
19Fc-1	GNGSYWYQVW
19Fc-2	GNGSYW
19Fc-3	GSYW
19Fc-4	GSYWYQVW
19Fc-5 (min19Fc)	GSYWYQVWF
19Fc-6	GYWYQVWF
19Fc-7	GWYQVWF
19Fc-8	GYQVW

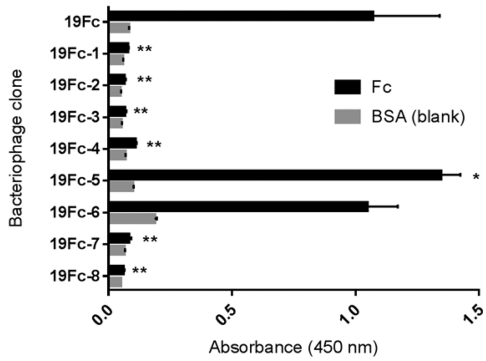

Figure 3. Relative affinities for hFc fragment of truncated phage-displayed peptides as compared in phage ELISA. Phages were contacted with immobilized hFc at 5×10^9 virions/well. Statistically significant differences in hFc binding (relative to the parent peptide 19Fc) are denoted by asterisks (one-way ANOVA followed by Bonferroni *post hoc* analysis; $*p < 0.05$ and $**p < 0.0001$, respectively).

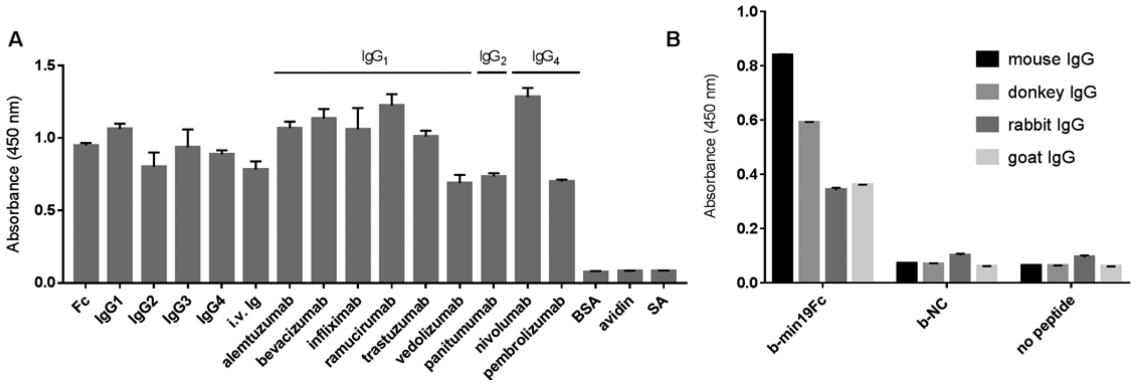

Figure 4. Reactivity of minimized peptide minFc19 with different IgGs. (A) Binding of phage displaying min19Fc to human IgG Fc, individual human IgG subclasses, a pool of human IgGs (i.v. Ig), and a set of different therapeutic monoclonal antibodies as assessed by qualitative phage ELISA assays. BSA, avidin, and SA were used as negative controls. (B) Binding of IgGs of different species to synthetic biotinylated peptide b-min19Fc complexed to immobilized SA. Unrelated synthetic peptide b-NC and SA alone were used as negative controls.

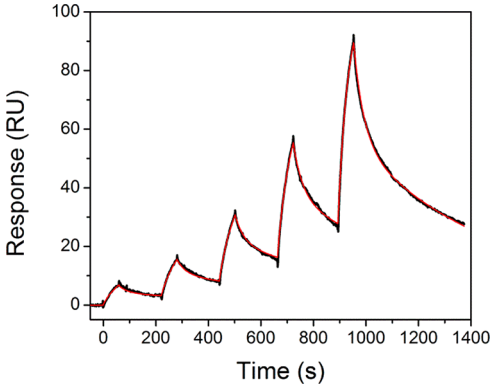

Figure 5. Single-cycle kinetic analysis of interaction between the human Fc fragment and the peptide b-min19Fc. For clarity, a single sensorgram is shown (black) along with the fitted curve (red). Binding curve was fitted using the bivalent analyte model. The experiment was performed in triplicate (Figure S4).

selective interaction of min19Fc with the Fc region. We estimated the *apparent* affinity of the biosensor surface for hFc to be in the submicromolar range (bivalent analyte model, K_{D1} = 652 ± 93 nM, K_{D2} = 5.87 ± 0.99 μM; three independent titrations). High affinity of the min19Fc for hFc can be attributed to the avidity effect, as there were up to four peptides coupled to each streptavidin molecule, a setting that simulates conditions encountered by antibodies on a peptide-functionalized affinity matrix during chromatography runs. Importantly, the SPR data along with the results from the experiment depicted in Figure 4B confirm that the synthetic peptide immobilized via a short linker retains the binding properties of the cognate phage-displayed ligand.

Construction and Characterization of Divalent Phage. Biacore analysis suggested that there are two peptide binding sites per Fc fragment. We thus hypothesized that linking two min19Fc peptides at an appropriate distance would result in a ligand with strongly enhanced binding compared to the peptide monomer. As the environment in which the interactions are monitored can significantly affect binding between partners, we decided to exploit the filamentous phage as a carrier also for display of a single and two min19Fc copies, respectively. This allowed for direct comparison of functional affinity for Fc among different display formats (i.e., depending on display valency). The approach was also more affordable in comparison to chemical synthesis of a large peptide (i.e., two copies of min19Fc separated by a long linker). To construct a divalent phage, one copy was directly displayed on filamentous virions fused to minor coat protein p3 via $(GGGGS)_3$/P3 coil-forming peptide linker (Figure S5A). The other min19Fc copy containing C-terminal $(GGGGS)_3$/P4 coil-forming peptide/His-tag/FLAG-tag appendix (Figure S5B) was separately expressed in *Escherichia coli* and purified. Both components were combined, which led to spontaneous association of P3–P4 coils[30] and consequently resulted in divalent display of

DOI: 10.1021/acs.bioconjchem.8b00395
Bioconjugate Chem. 2018, 29, 2763–2775

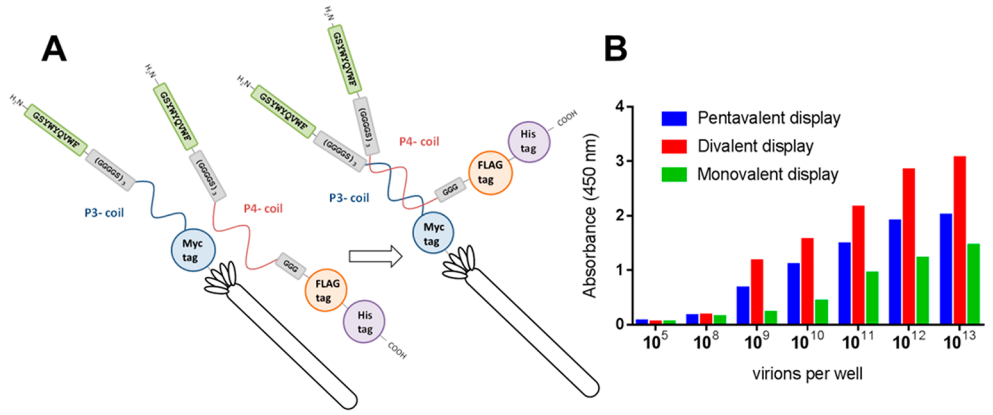

Figure 6. Design and characterization of divalent phage. (A) Schematic representation of divalent phage formation. (B) Comparative binding of mono-, di-, and pentavalent min19Fc-displaying phage particles to human IgG as analyzed by phage ELISA.

Name	Sequence
min19Fc	GSYWYQVWF
min19Fc-4A	GSY**A**YQVWF
min19Fc-5A	GSYW**A**QVWF
min19Fc-6A	GSYWY**A**VWF
min19Fc-7A	GSYWYQ**A**WF
min19Fc-8A	GSYWYQV**A**F

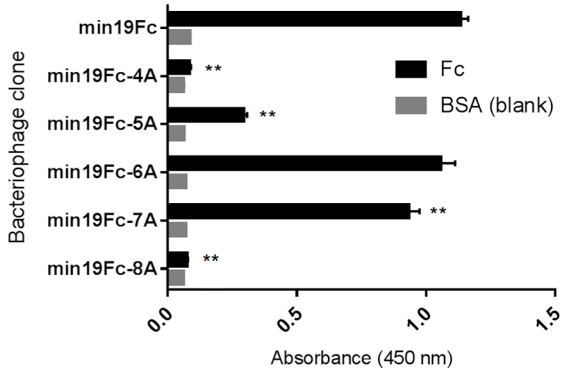

Figure 7. Relative affinities for hFc fragment of phage-displayed peptides with individual residues substituted for alanine as compared in phage ELISA. Phages were contacted with immobilized hFc at 5×10^9 virions/well. Statistically significant differences in Fc binding (relative to the parent peptide min19Fc) are denoted by asterisks (one-way ANOVA followed by Bonferroni *post hoc* analysis; $^{**}p < 0.0001$, respectively, compared with the min19Fc clone).

min19Fc on phagemid virions (Figure 6A). Divalent virions were purified by double polyethylene glycol (PEG)/NaCl precipitation to remove the excess free recombinant peptide and subjected to quantitative phage ELISA in comparison to pentavalent min19Fc-M13KBE phages and monovalent min19Fc phagemid virions (Figure 6B). As presumed, divalent virions displayed stronger binding to immobilized Fc compared to monovalent particles. Importantly, they also outperformed pentavalent phages, indicating the importance of appropriate distance between the two peptide ligands for simultaneous interaction with the single IgG molecule. The linker length (~10 nm; twice that of $(GGGGS)_3$ assuming 3.5 Å per residue of extended peptide chain) was chosen upon inspection of crystallographic structures of IgGs from the Protein Data Bank (1FC2,[27] 1DN2,[24] and 3D6G[31]) and may not be optimal.

Alanine Scanning of min19Fc Peptide. We subjected the peptide min19Fc to alanine scanning in order to assess the contribution of its individual amino acid residues to hFc binding. Five variants with alanine substitutions were designed (Figure 7) and displayed on the M13KBE phage. Phage clones were subjected to phage ELISA, and the affinities of individual peptide variants to hFc were compared to that of the parent peptide min19Fc. Substitutions of Trp4 and Trp8, as well as Tyr5 (numbering according to min19Fc parent peptide) strongly affected binding to hFc, whereas substitutions of Gln6 and Val7 were tolerated with no or only a minor loss of binding affinity. Tyr3 and Phe9 were confirmed as essential for Fc binding in trimming analysis (Figure 3), while residue Gly1 is the result of a restriction site "scar" (Figure S3).

Characterization of Charged Variants of min19Fc. Truncating analysis (Figure 3) and alanine scanning (Figure 7) identified aromatic amino acid residues in min19Fc (Tyr3, Trp4, Tyr5, Trp8, and Phe9) as crucial for Fc fragment binding. Even though valine is structurally similar to alanine, substitution of Val7 with alanine resulted in a minor loss of binding activity (Figure 7). We therefore focused on modifying position 6 occupied by glutamine in parental peptide min19Fc with the goal of augmenting peptide's solubility and possibly potentiating the pH dependence of its interaction with the Fc fragment. Gln6 was substituted with charged residues (aspartate, glutamate, or lysine) yielding peptides min19Fc Q6D, min19Fc Q6E, and min19Fc Q6K, respectively, and the peptides were displayed on the phage. We analyzed binding properties of modified peptides in quantitative phage ELISA in comparison with the parental peptide min19Fc (Figure 8A) and noted significant differences in concentration dependent binding of individual phage clones to human IgGs. Whereas all three newly designed peptides retained binding to the Fc fragment, substitutions of Gln6 with negatively charged residues resulted in peptides with improved binding affinity for IgG.

DOI: 10.1021/acs.bioconjchem.8b00395
Bioconjugate Chem. 2018, 29, 2763−2775

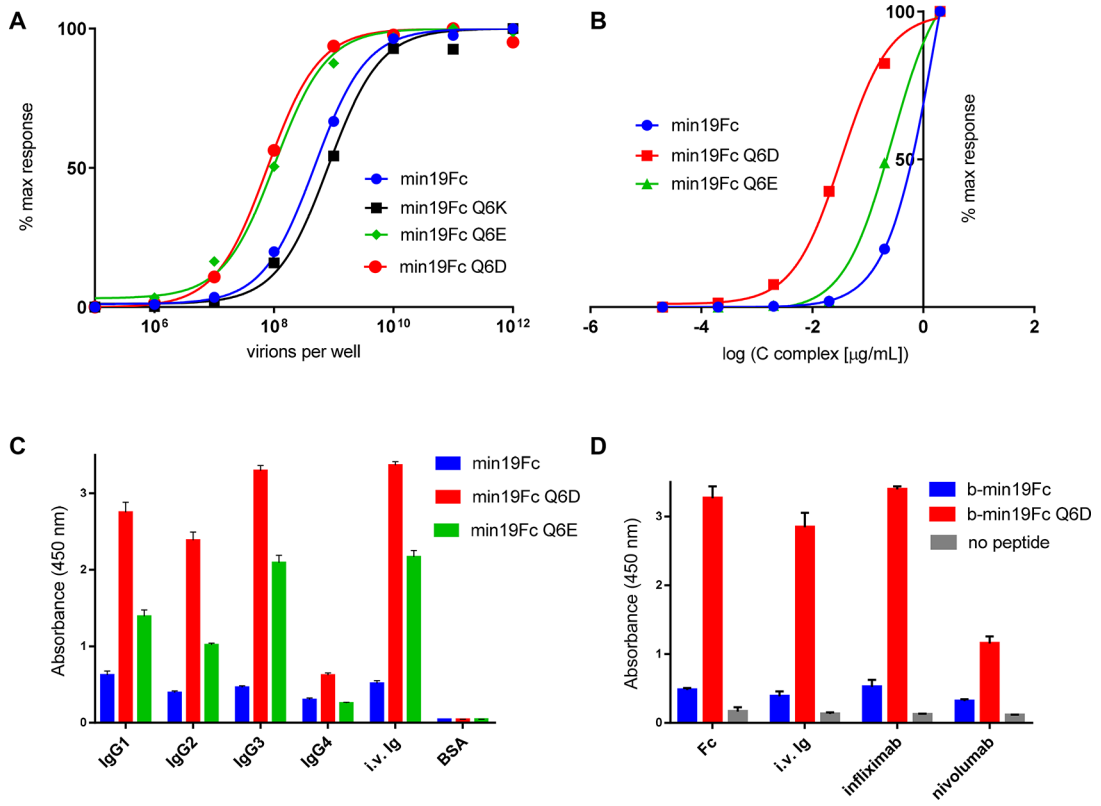

Figure 8. Characterization of charged variants of min19Fc. (A) Relative binding of phage clones displaying min19Fc and its charged variants with amino acid substitutions at position 6 to human IgGs as assessed by phage ELISA assay. (B–D) Relative binding of complexes, comprised of synthetic peptides b-min19Fc, b-min19Fc Q6D, or b-min19Fc Q6E and SA-HRP conjugate, to a pool of human IgGs (B), to human IgGs of different subclasses and a mixture thereof (i.v. Ig; C), and to therapeutic monoclonal antibodies infliximab and nivolumab, hFc, and i.v. Ig (D). Unrelated synthetic peptide b-NC and SA-HRP alone (no peptide) were used as negative controls. Experiments in C and D were performed in triplicate.

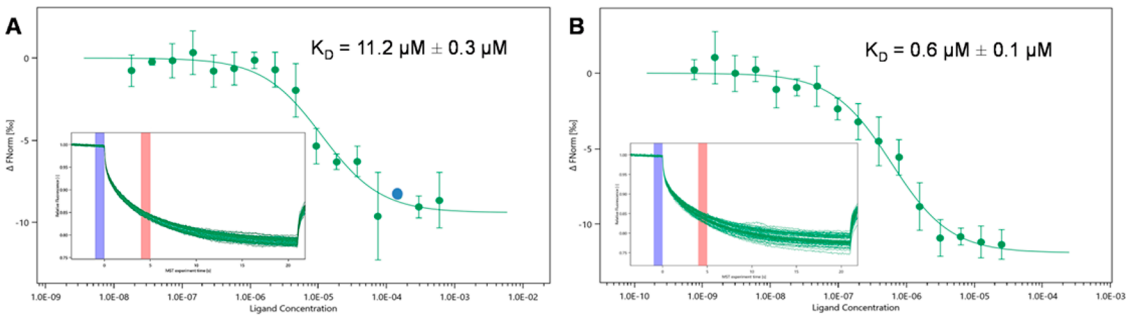

Figure 9. MST analyses of min19Fc (A) and min19Fc Q6D (B) binding to human IgGs. The insets show MST traces from which sigmoidal dose–response curves of peptides titrated against fluorophore-labeled human IgGs were derived. The average K_D values ± SD were calculated from four experimental replicates. In the min19Fc MST binding curve, outliers were observed at a single peptide concentration (150 μM; not shown), likely due to precipitation of the peptide. Thus, at this ligand concentration, only a single measurement could be used for dose–response curve construction (denoted by blue dot). F_{Norm}, normalized fluorescence; ligand concentration in mol/L.

The high affinity peptides (min19Fc Q6D, min19Fc Q6E) and the parent min19Fc were chemically synthesized and C-terminally coupled to biotin via short linkers. The biotinylated peptides were complexed with the SA-HRP conjugate; serial dilutions were contacted with human IgG-coated microtiter wells (Figure 8B), and binding was detected with peroxidase chromogenic substrate. Peptides harboring negatively charged residues at position 6 displayed higher affinity for IgG compared to parental minimized peptide min19Fc, with aspartate being preferred over glutamate. In addition, the binding of synthetic peptides to four human IgG subclasses was qualitatively assessed in a similar manner (Figure 8C). All three peptides bound to human IgGs of all four subclasses, showing the lowest affinity for IgG_4. In agreement with previous observations, the binding affinity of both negatively charged variants was higher compared to the parental synthetic peptide b-min19Fc. Finally, we compared the binding activity of synthetic peptide b-min19Fc Q6D (vs b-min19Fc) to therapeutic monoclonal IgGs infliximab (chimeric IgG_1) and nivolumab (human IgG_4) by tethering it to a SA-HRP conjugate and contacting the complex with antibody-coated wells (Figure 8D). The improved peptide reacted more

DOI: 10.1021/acs.bioconjchem.8b00395
Bioconjugate Chem. 2018, 29, 2763–2775

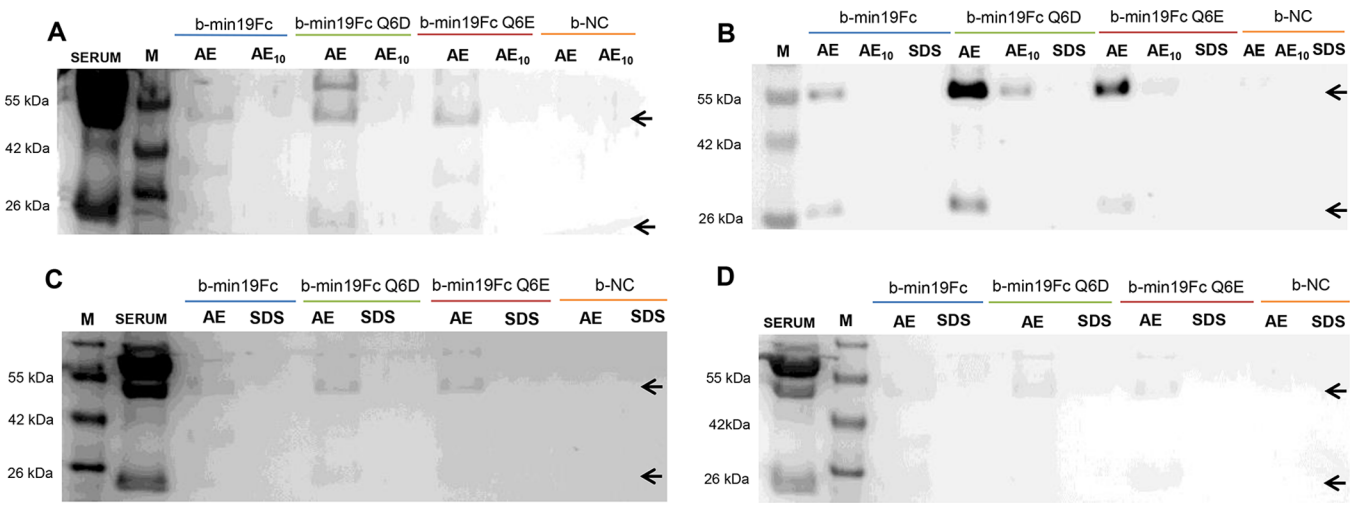

Figure 10. Isolation of IgGs from human serum in pull-down experiments with synthetic peptides. (A) Coomassie stained SDS-PAGE gel showing pulled-down material. (B) Western blot analysis of pulled-down material. Peptide b-NC was used as the negative control. AE, acidic elution; AE_{10}, 10-fold diluted acidic eluate; SDS, elution with SDS-PAGE loading dye at 100 °C; M, protein marker. (C and D) Same experiments as in A, but the beads were washed with buffer containing either 1 M NaCl (C) or 0.5 M sodium caprylate (D). The arrows indicate positions of bands corresponding to heavy and light chains of IgG.

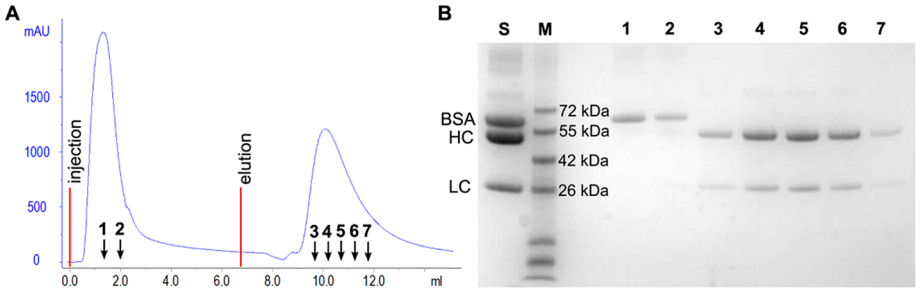

Figure 11. Chromatogram (A; absorbance at 280 nm) and the corresponding Coomassie stained gel (B) after SDS-PAGE analysis of fractions collected during chromatographic separation of human IgGs and BSA from PBS using min19Fc Q6D-functionalized affinity matrix. Lane S, 1:10 dilution of loading material; lane M, protein marker; lanes 1 and 2, flow-through; lines 3 to 7, eluted material corresponding to antibody heavy (HC) and light chains (LC). The samples were analyzed under reducing conditions.

strongly with infliximab than nivolumab and outperformed the parent peptide min19Fc, which is in agreement with previous findings (Figure 8A–C).

Microscale Thermophoresis. The microscale thermophoresis (MST) method is based on the ligand binding-induced change in movement of fluorescent molecules across a temperature gradient, allowing for rapid detection of a wide range of biomolecular interactions.[32] We used MST to quantitate the binding affinity of peptides min19Fc and min19Fc Q6D to a fluorophore-labeled human IgG pool (Figure 9). The averaged dissociation constants (K_D) of peptides b-min19Fc and min19Fc Q6D for IgG binding were determined to be 11.2 ± 0.3 μM and 0.6 ± 0.1 μM, respectively. The observed ~18-fold higher affinity of the min19Fc Q6D peptide is consistent with previous semi-quantitative analyses (Figure 8). The affinity of peptide min19Fc for IgG determined with MST was lower compared to the one estimated by SPR analysis. This can be explained by the fact that in a MST binding study, no avidity effects were present as IgGs were titered with peptides in monomeric form in solution. Thus, K_D determined with SPR represents *apparent* affinity as opposed to *true* affinity measured by MST analysis.

Pull-down Assays. Pull-down assays with synthetic peptides were undertaken to confirm that their interactions with IgGs are strong enough to support antibody isolation from complex mixtures, as well as to assess the peptides' specificity. Biotinylated peptides b-min19Fc, b-min19Fc Q6E, and b-min19Fc Q6D were coupled to streptavidin paramagnetic beads and used to pull down IgGs from human serum. Eluted material was analyzed by SDS-PAGE followed by Coomassie staining (Figure 10A) and Western blot (Figure 10B). IgGs were enriched with all three peptides but not with b-NC control peptide. Peptide min19Fc Q6D captured significantly more IgGs than min19Fc and min19Fc Q6E (compare band intensities in Figure 10B) but also bound more serum albumin (HSA; Figure 10A). Sequential elution in SDS-PAGE loading dye at 100 °C showed that elution with pH shock was quantitative (Figure 10B). To limit nonspecific binding of HSA to peptide-functionalized beads, we added either 1 M NaCl (Figure 10C) or 0.5 M sodium caprylate (Figure 10D) to the washing buffer and repeated the experiments. Peptides min19Fc Q6D and min19Fc Q6E, being highly hydrophobic and carrying negatively charged carboxyl groups, resemble fatty acids that are bound by albumin. We speculated that saturating fatty acid binding sites on HSA with caprylate would interfere with peptide binding, whereas a high salt concentration would disrupt electrostatic interactions (but promote hydrophobic interactions).[33] Both

DOI: 10.1021/acs.bioconjchem.8b00395
Bioconjugate Chem. 2018, 29, 2763–2775

additives reduced nonspecific binding of HSA to peptide-functionalized beads.

Chromatographic Evaluation of Peptide Ligand. N-terminally acylated peptide min19Fc Q6D with the amidated GGDDK-NH_2 C-terminal extension to promote solubility and provide a single reactive primary amine was coupled to a CNBr-activated Sepharose matrix at ∼15.6 μmol/mL of settled slurry. The peptide-functionalized sepharose was packed into a small chromatographic column housing. PBS was spiked with human i.v. IgG and BSA (2 mg/mL each) and injected onto the affinity column. Following washing with PBS supplemented with 1 M NaCl, bound material was recovered in elution buffer (50 mM Gly·HCl, pH to 2.5; Figure 11A) and analyzed by SDS-PAGE (Figure 11B). The column-bound fraction was highly enriched in IgGs, indicating high selectivity of the min19Fc Q6D-functionalized matrix for antibodies over albumin. Moreover, no antibodies were detected in flow-through fractions, which further confirms highly specific binding of antibodies and indicates that the binding capacity of the column exceeds 2 mg of IgG (i.e., ∼ 7.4 mg IgG/mL). The marked increase in purity of eluted IgGs compared to the pull-down experiment (Figure 10C) can be attributed to a different surface chemistry of the affinity matrix, as well as to more effective washing accomplished in the column format.

We set out to determine the dynamic binding capacity (DBC) of the min19Fc Q6D-functionalized column. Since the column volume was very small (∼0.27 mL), exact determination of void volume, required for calculation of DBC, was impossible. We therefore took an alternative approach. Equal volumes of increasing IgG concentrations were injected into the FPLC system bypassing the column, and corresponding peaks were integrated to calculate the areas under the curve (AUC) and plot a standard curve (Figure S6). Next, a high concentration of IgGs (5 mg/mL, ensuring column overloading) was injected onto the affinity column and, after thorough washing, eluted with elution buffer. The amount of column-captured IgG was calculated from the AUC of the eluted peak using the standard curve. The DBC of the affinity column estimated in three successive runs was 11.0 ± 1.5 mg IgG/mL. It should be noted that the column construction and the reported IgG separation represent initial proof-of-concept experiments and have not been extensively optimized.

We subjected our column to human IgG purification from a spiked growth medium (Figure S7A) and crude human serum (Figure S7B) and attained antibodies with purities exceeding 95% (according to densitometric analyses of Commassie stained eluted fractions), which is comparable to affinity resins reported by Verdoliva et al.,[12] Zhao et al.,[34] and Yang et al.,[14] as well as SpA-based chromatography.[12,21] Although we did not systematically analyze column stability, we observed no significant reduction of its functional performance over more than 25 chromatographic runs.

Many factors are known to influence the purification yield and the degree of isolated IgG purity, such as differences in flow rate, ligand density, feedstocks, chromatographic buffers, and matrix types, preventing direct comparison of our column to other reported affinity resins. For example, Zhao et al.[34] systematically analyzed the performance of sepharose affinity matrices functionalized with their SpA mimetic octapeptide at four different densities (over the 3-fold range from 10.4 to 31.0 μmol/mL) and observed significant differences in DBC values (14.5 to 30.5 mg/mL) using human serum as a feedstock. Yang et al.[14] noted that the density of their hexapeptide ligand coupled to a metacrylate matrix significantly affected the affinity of human IgG and specificity for the Fc fragment, thereby determining recovery and purity of IgG isolated from a spiked growth medium. Preliminary data indicate that the DBC of our prototype column (i.e., ∼11 mg/mL) is lower compared to some affinity matrices reported previously (e.g., up to 60 mg/mL for D-PAM[21] or up to 30 mg/mL for SpA mimetic peptide[34]). However, we expect that, with optimization of ligand density and chromatographic conditions, an improved purification process can be achieved.

CONCLUSION

We report here the development of a set of simple peptides that bind to the Fc region of all human IgG subclasses. When coupled to paramagnetic beads or a chromatographic matrix, the peptides were shown to selectively enrich antibodies from complex protein mixtures. Elution with pH shock was employed in each case, resembling elution requirements for SpA-based matrices. It should be stressed that elution conditions were kept constant from phage library screening onward, and no attempts were made to optimize them at this stage. However, the main advantages (besides economic ones) of adopting the peptide ligand rather than SpA for antibody affinity chromatography are the expected lack of peptide immunogenicity (which can be problematic in the case of ligand leaching) and stability under harsh sanitation conditions. In addition, relatively simple modifications of peptide ligands can be undertaken to increase their resistance to proteases. For example, we have pulled-down antibodies from human serum with the retro-inverso analogue of min19Fc, although slightly less efficiently compared to min19Fc (not shown). Furthermore, SpA lacks affinity for certain immunoglobulins such as human IgG3. The broad specificity of reported peptide ligands for IgG (Figures 4 and 8) can be considered a favorable property in antibody purification. Antibodies are typically produced by hybridoma or recombinant DNA technology and thus represent the only IgG present in the growth medium, allowing the use of a universal affinity column in downstream processing.

The structure-analysis study of our lead peptide provides the basis for further rational development of peptide ligands with tailored properties. For example, high affinity of peptides might be secondary to their binding specificity in affinity chromatography. In fact, if the ligand affinity is too high, this will necessitate elution of bound material under conditions that jeopardize its integrity. On the other hand, high binding capacity of resin functionalized with moderate-affinity ligands can still be achieved by increasing ligand density. Another goal of modification might be to increase the water solubility of synthetic peptides in order to simplify their coupling to a chromatographic matrix. Our current efforts are focused on elucidating the mechanism of IgG−peptide ligand interaction, and optimization of chromatographic conditions (i.e., ligand density, choice of binding, and elution buffers). In addition to affinity chromatography, the peptides might find use in applications such as homogeneous IgG immobilization (e.g., on biosensor surfaces or pull-down matrices) and noncovalent (indirect) labeling of antibodies (e.g., formation of noncovalent antibody−drug complexes).

DOI: 10.1021/acs.bioconjchem.8b00395
Bioconjugate Chem. 2018, 29, 2763−2775

MATERIALS AND METHODS

Materials. PhD phage display libraries (PhD-7, PhD-12, and PhD-C7C) were purchased from New England Biolabs (NEB, Ipswich, MA, USA). Human Fc fragment (hFc) and immunoglobulin G subtypes (IgG_1, IgG_2, IgG_3, and IgG_4) were procured from Athens Research & Technology (Athens, GA, USA). Streptavidin-coated (MyOne Streptavidin T1) paramagnetic beads were from Thermo Fisher Scientific (Rockford, IL, USA). Anti-M13 horseradish peroxidase (HRP)-conjugate and streptavidin-HRP (SA-HRP) conjugate were acquired from GE Healthcare (Little Chalfont, UK) and GenScript Corp (Piscataway, NJ, USA), respectively. Custom oligonucleotides were procured from Sigma-Aldrich (St. Louis, MO, USA). gBlock synthetic gene fragments were produced by Integrated DNA Technologies (IDT, San Jose, CA, USA), and peptides were synthesized by Innovagen AB (Lund, Sweden). Phagemid phage display vector pIT2, helper phage KM13, and bacterial host strain *Escherichia coli* TG1Tr were obtained from Source BioScience (Nottingham, UK). *E. coli* BL21 (DE3) pLysS bacterial expression strain and plasmid pET28a(+) were purchased from Merck (Burlington, MA, USA). CNBr-activated sepharose 4B was purchased from Sigma-Aldrich.

Screening of Phage Display Libraries. A human Fc fragment was randomly biotinylated via primary amines using EZ-Link Sulfo-NHS-Biotin (Thermo Fisher Scientific) according to the manufacturer's instructions. Three phage display libraries of linear and cyclic random peptides were subjected to separate biopanning processes against the biotinylated human Fc fragment (b-hFc). In the first selection round, libraries were incubated with 7 μg of b-hFc for 12 h before capturing b-hFc–phage complexes onto streptavidin-coated paramagnetic beads (in subsequent rounds, contact time was shortened to 1 h). Nonbound phages were discarded using 10 washing steps with PBS containing 0.05% Tween-20 (PBST)/0.1% BSA. In the last washing step, biotin (20 μM) was added to the wash buffer. Bound phage was eluted with pH shock (0.2 M Gly·HCl, pH 2.2) for 10 min, and the eluate was immediately neutralized with 1 M Tris·HCl, at pH 9.1. Phages were amplified by infecting the *E. coli* ER2738 host strain and isolated by double PEG/NaCl precipitation. To increase stringency, the amount of b-hFc was reduced to 1 μg and 300 ng in the second and third selection rounds, respectively, and beads were washed 15 times with 0.1% PBST/0.1% BSA. To avoid enrichment of streptavidin-binding peptides, input phages for the second and third selection rounds were exposed to streptavidin beads for 1.5 h before they were contacted with b-hFc. From the second round on, parallel affinity selections were performed in which phages were eluted either non-specifically (with pH shock) or competitively (displacement with 100 μL of 52 μg/mL hFc). After each round, a small amount of eluate was titered to monitor the selection progress (percentage of eluted virions relative to the input was calculated).

Polyclonal Phage ELISA. Wells of the MaxiSorp microtiter plate (Thermo Fisher Scientific) were coated overnight at 4 °C with 50 μL of either hFc or streptavidin at 5 μg/mL. Next, the wells were blocked with 2% BSA in PBS for 1 h at room temperature and washed with 0.1% PBST. Amplified phages from eluates of selection rounds 1 to 3 containing 5×10^{10} pfu in 100 μL of 0.1% BSA/0.05% PBST were added to wells and incubated for 1 h with gentle agitation. After extensive washing, bound phages were detected with HRP-conjugated anti-M13 monoclonal antibodies and the chromogenic substrate 3,3′,5,5′-tetramethylbenzidine (TMB). After color development, enzymatic reaction was stopped by adding 2 M H_2SO_4, and absorbance was recorded at 450 nm.

Functional Testing and Sequencing of Positive Clones. Forty phage clones from the last selection round were randomly chosen; 20 clones were collected from the competitive and 20 from the nonspecific elution pool. Monoclonal ELISA was performed essentially as described above, except that amplified phage clones were not purified and titered; instead, clear culture supernatants diluted 1:1 in 100 μL of 0.5% BSA/0.1% PBST were incubated in hFc-coated and blank wells. Phage clones were considered selective Fc binders if signal-to-background ratio (i.e., binding to hFc- vs BSA-coated (blank) wells) was ≥4. Single stranded phage DNA of positive clones was isolated by precipitation with ethanol after the capsid proteins were denatured with 4 M sodium iodide. Inserts encoding the displayed peptides were sequenced by GATC Biotech (Konstanz, Germany) using the −96 gIII sequencing primer (5′-CCCTCATAGT-TAGCGTAACG-3′). Furthermore, individual phage clones were reamplified, and 1×10^{10} virions/well were subjected to phage ELISA as described above to semiquantitatively compare the affinities.

Monovalent Display of Peptides and Quantitative Phage ELISA Assay. Fc-binding peptides 6Fc, 14Fc, 19Fc, and 20Fc were displayed on phages in a monovalent format using the 3 + 3 display approach.[35] Synthetic complementary oligonucleotides encoding the displayed peptides (Table S2) were mixed in equimolar ratio, annealed together by heating to 95 °C and slowly cooling down to room temperature, and ligated into *Nco*I/*Not*I digested pIT2 phagemid vector. Recombinant phagemids were introduced into chemically competent *E. coli* TG1Tr cells by the standard heat shock procedure, and phages were rescued by superinfection with KM13 helper phage. Upon isolation with PEG/NaCl precipitation, phage clones were quantified spectrophotometrically using the following equation (derived from measurements of Day and Wiseman[36]):

$$\frac{\text{virions}}{\text{mL}} = \frac{(A_{269} - A_{320}) \times 6 \times 10^{16}}{\text{number of bases/virion}}$$

and subjected to phage ELISA at increasing concentrations (10^5, 10^9, 10^{10}, and 10^{11} virions/well) to assess the relative affinities of displayed peptides for hFc.

Competitive Phage Fluorescence-Linked Immunosorbent Assay (Phage FLISA). Freshly amplified bacteriophage clone 19Fc was isolated from 20 mL of bacterial culture supernatant by double PEG/NaCl precipitation and ultimately resuspended in 200 μL of 0.1 M sodium bicarbonate buffer, at pH 8.9. Forty microliters of 1 mg/mL fluorescein isothiocyanate (FITC; Sigma-Aldrich) in DMSO was gradually added in 8 μL aliquots to the phage suspension at 5 min intervals during continuous shaking protected from light. After the last addition of FITC, the reaction mixture was shaken for another hour in the dark at room temperature. Fluorescein-labeled bacteriophages were purified by double PEG/NaCl precipitation to remove excess FITC and resuspended in 200 μL of PBS.

Competition of FITC-labeled 19Fc phage with staphylococcal immunoglobulin-binding protein A (SpA) for hFc binding was assessed by phage FLISA assay. Briefly, hFc-coated

DOI: 10.1021/acs.bioconjchem.8b00395
Bioconjugate Chem. 2018, 29, 2763−2775

and BSA-blocked black MaxiSorp microtiter plate wells were filled with 100 μL of 0.1% PBST containing 1.2×10^{10} of FITC-labeled phage particles and an increasing concentration (10 nM, 100 nM, or 1 μM) of SpA. After 1 h, the well contents were discarded; the wells were extensively washed with 0.1% PBST and finally filled with 50 μL of PBS. Fluorescence intensities were measured at 525 nm upon excitation at 495 nm (10 nm bandwidths) with a Tecan Safire microtiter plate reader (Tecan Group AG, Mannedorf, Switzerland). Signals from blank (BSA-coated) wells were subtracted from fluorescence values of paired test wells. The experiment was performed in triplicate.

Minimization of 19Fc Parent Peptide by Truncation. To evaluate the minimal sequence requirements of the parent peptide 19Fc for Fc binding, we designed a series of N- and C-terminally truncated variants (labeled 19Fc-1 through 8; Figure 3). The peptides were displayed fused to the minor capsid protein p3 encoded by a modified M13KE phage vector (termed M13KBE; Supporting Information Methods). M13KBE was constructed to allow convenient subcloning of annealed short synthetic complementary oligonucleotides encoding peptides to be displayed (Table S3) and contains an additional *Bsp*EI restriction site between the *Eag*I and *Kpn*I (Figure S3). Affinities of the truncated peptides for hFc binding (relative to that of the parent peptide 19Fc) were assessed by phage ELISA assay. The experiment was performed with 5×10^9 virions/well of each phage clone in triplicate.

Reactivity of minFc19 with Different IgGs. The ability of phage-displayed peptide min19Fc to bind to a number of therapeutic monoclonal antibodies and human IgG of individual subclasses was checked by qualitative phage ELISA assay as described above; phage particles were contacted with immobilized antibodies at 5×10^9 virions/well.

Synthetic biotinylated peptide min19Fc (b-min19Fc; GSYWYQVWFGGGSKKK(ε-biotin)-$CONH_2$) was coupled to streptavidin (2 μg/mL in PBS) at a 4:1 molar ratio, and the complex was coated onto the microtiter plate wells. A biotinylated peptide with an amino acid sequence unrelated to min19Fc (b-NC; GNWTLGGYKGK(ε-biotin) (head-to-tail cyclized)[37]) and uncomplexed streptavidin were used as negative controls. Coated and blocked wells were reacted with conjugates of HRP and IgGs of different species (monoclonal *mouse* anti-M13-HRP (GE Healthcare, Little Chalfont, UK), polyclonal *donkey* antigoat-HRP (Santa Cruz Biotechnology, Dallas, USA), polyclonal *rabbit* antisheep-HRP (Jackson Immuno Research, West Grove, PA, USA), and polyclonal *goat* antimouse-HRP (Milipore, Billerica, MA, USA)), and binding was detected with TMB.

Surface Plasmon Resonance Analysis of Peptide min19Fc:hFc Interaction. The interaction between the b-min19Fc and human Fc fragment was analyzed by surface plasmon resonance using Biacore X100 (GE Healthcare Life Sciences, Chicago, IL, USA) at 25 °C. Streptavidin was immobilized on the surface of a CM5 chip via amine coupling using EDC (N-ethyl-N-(3-diethylaminopropyl) carbodiimide)/NHS (*N*-hydroxysuccinimide) chemistry according to the manufacturer's recommendations to achieve a stable response of approximately 4000 resonance units (RU). Remaining unreacted groups were blocked with ethanolamine. To immobilize the peptide onto the chip, 120 nM solution of b-min19Fc was injected over the sensor chip until a stable response of approximately 250 RU was attained. SPR measurements were performed by using the kinetic titration approach, i.e., sequential injections of increasing concentrations of the analyte over a functionalized sensor chip surface, omitting regeneration steps between injections. Five sequential increasing concentrations of hFc solution (10 nM, 20 nM, 40 nM, 80 nM, and 160 nM) in running buffer (PBS buffer with 0.005% P20) were fluxed over the sensor chip surface for 60 s at a flow rate of 30 μL/min, followed by a final 160 s dissociation with running buffer. Between replicates, the surface was regenerated with two sequential 18 s injections of 1 mM NaOH. The uncoated reference surface was used to correct for systematic noise and instrument drift. The binding assay also included three start-up cycles using buffer to equilibrate the surface, as well as a zero concentration cycle of analyte in order to obtain a blank response usable for double reference subtraction. BiaEvaluation software 3.2 (GE Healthcare) was used for curve fitting and extraction of kinetic parameters from SPR data. Raw data were fitted by different predefined models, and the bivalent analyte model was best suited for the analyzed interaction (i.e., it gave the best fit).

Divalent Phage Construction and Evaluation. Peptide min19Fc was displayed on the phage in a divalent format by exploiting the heteromeric P3/P4 coiled coil system (Figure 6A). The min19Fc-P3 coil-p3 fusion was expressed from the pIT2 phagemid display vector. KM13-rescued phagemid virions were combined with soluble min19Fc-P4 peptide fusion expressed in *E. coli* (Supporting Information Methods). Peptides P3 and P4 spontaneously dimerize with high selectivity,[30] allowing the display of two copies of min19Fc on a single phage particle. We inserted relatively long flexible peptide linkers ($(GGGGS)_3$) between min19Fc and P3/P4 coils to allow for concomitant binding of both Fc ligands to a single IgG molecule.

The functional avidity of divalent phages was evaluated by quantitative phage ELISA in direct comparison with mono- and pentavalent phages (i.e., 3 + 3 phagemid-based and three phage vector-based display platforms,[35] respectively). Increasing phage concentrations (10^5, 10^8, 10^9, 10^{10}, 10^{11}, 10^{12}, and 10^{13} virions/well) were incubated in wells coated with a pool of human IgGs (i.v. IgG, Octagam; Octapharma), and bound phages were detected using the anti-M13-HRP conjugate and TMB. The background absorbances (phages incubated in BSA-coated wells) were subtracted from the paired test wells.

Alanine Scanning. To assess the contribution of each residue of the minimized peptide min19Fc to hFc binding affinity, we designed a series of min19Fc variants with alanine replacing individual residues (Figure 7 and Table S3). The peptides were displayed fused to the minor capsid protein p3 of M13KBE as described above. The affinities of peptide variants for Fc binding (relative to min19Fc) were assessed by phage ELISA assay as described above. The experiment was performed with 5×10^9 virions of each phage clone in triplicate.

Characterization of Charged min19Fc Variants. In an attempt to increase the solubility of peptide min19Fc, we replaced the nonessential residue Gln6 with charged residues. Variants of the min19Fc peptide with Q6D, Q6E, and Q6K substitutions (Table S3) were displayed on the M13KBE phage, and their affinities for human IgGs were assessed by phage ELISA relative to the parent clone min19Fc as described above. Signals produced by phages at different concentrations (10^7, 10^8, 10^9, 10^{10}, 10^{11}, and 10^{12} virions/well) were recorded,

DOI: 10.1021/acs.bioconjchem.8b00395
Bioconjugate Chem. 2018, 29, 2763−2775

and background signals (from BSA-coated wells) were subtracted from absorbances of paired test wells.

Peptides min19Fc, min19Fc Q6D, and min19Fc Q6E were synthesized with a C-terminal GGGSK(ε-biotin)-$CONH_2$ appendix, and their binding activities were evaluated in an assay akin to ELISA. Microtiter plate wells were coated with a pool of human IgGs and blocked with BSA. Biotinylated synthetic peptides and the SA-HRP conjugate were mixed in advance at a molar ratio of 4:1 to formulate tetrameric $(peptide)_4$:SA-HRP complexes. Complexes were sequentially diluted and added to IgG-coated wells such that the SA-HRP concentration was in the range of 20 pg/mL to 2 ng/mL. After gentle shaking for 1 h, the wells were extensively washed, and bound complexes were detected with TMB.

Additionally, we assessed relative binding affinity of synthetic biotinylated peptides b-min19Fc and b-min19Fc Q6D to therapeutic monoclonal antibodies infliximab (chimeric IgG_1; Remsima; Celltrion, Incheon, South Korea) and nivolumab (human IgG_4; Opdivo; Bristol-Myers Squibb, Uxbridge, UK), human IgGs of different subclasses (IgG_1, IgG_2, IgG_3, and IgG_4), and a mixture thereof (human i.v. IgG). Peptides were complexed to the SA-HRP conjugate to a final concentration of 1 ng/mL and contacted with target-coated microtiter plate wells. $(b\text{-}NC)_4$/SA-HRP and SA-HRP conjugate alone (i.e., not coupled to peptides) were used as negative controls.

Microscale Thermophoresis. Interactions between human IgGs and synthetic peptide affinity ligands min19Fc and min19Fc Q6D were studied with microscale thermophoresis (MST) on Monolith NT.115pico red (Nanotemper Technologies, Munich, Germany). Human IgGs were labeled with fluorescent dye NT-647 using the Monolith NT Protein Labeling Kit RED-NHS (Nanotemper Technologies) according to the manufacturer's instructions. The concentration of labeled antibody (3.5 nM) was chosen such that observed fluorescence was approximately 6000 units at medium MST power (40%). Peptides were dissolved in water and later diluted in water with 0.05% Tween 20 and 1 mg/mL BSA. Labeled antibodies were diluted in the same diluent and were added to serially diluted peptide aliquots (for min19Fc ranging from 595 μM to 18.2 nM and for min19Fc Q6D ranging from 25 μM to 763 pM) in 1:1 volumetric ratio. The samples were loaded into standard capillaries and incubated for 10 min at room temperature. All measurements were taken at 20 °C using medium MST power and 10% excitation power. Experiments were performed with four replicates. Binding affinity (K_D) was derived by analyzing the change in normalized fluorescence (F_{norm}= fluorescence after thermophoresis/initial fluorescence) as a function of peptide concentration. Data processing and curve fitting were performed using NanoTemper Analysis software.

Pull-down Assays. A total of 800 ng of biotinylated synthetic peptides b-min19Fc, b-min19Fc Q6E, or b-min19Fc Q6D were coupled to 0.5 mg of streptavidin-coated paramagnetic beads. Beads coupled with b-NC were used as the negative control. Functionalized beads were used for pull-down experiments from 100 μL of intact human sera diluted 1:1 in 100 μL of 0.1% PBST, where extensive washing with either 0.1% PBST or PBST supplemented with 1 M NaCl or 0.5 M sodium caprylate was applied. Bound material was sequentially eluted in 50 μL of 0.2 M Gly·HCl, at pH 2.2 (10 min at room temperature), and 50 μL of SDS-PAGE loading dye containing 0.1% SDS and 150 mM DTT (5 min at 100 °C) and analyzed by SDS-PAGE and Western blot.

Affinity Chromatography. Synthetic peptide min19Fc Q6D (Ac-GSYWYDVWFGGDDK-NH_2) was coupled to a cyanogen bromide-activated Sepharose 4B matrix via the ε-NH_2 group of lysine. Briefly, 280 mg of dry CNBr-activated sepharose powder was suspended in 1 mL of cold 1 mM HCl and swollen for 5 min. The slurry was washed with 60 mL of cold 1 mM HCl in a disposable 5 mL gravity column over 30 min and then with 6 mL of cold distilled water and finally with 6 mL of cold coupling buffer (0.1 M Na_2CO_3, 0.5 M NaCl, pH 9.5). A total of 270 μL of gel was added to 2.4 mL of peptide solution (5 mg/mL) in a coupling buffer, and the mixture was incubated for 2 h at room temperature on a shaker. Tricorn 5/20 column (GE Healthcare) was packed with the functionalized slurry and connected onto an Äkta Explorer 10S chromatography system (GE Healthcare). The excess peptide was washed away with coupling buffer, and the column was washed with distilled water. Unreacted CNBr groups were blocked with 1 M ethanolamine, at pH 8.0, for 2 h at room temperature at a flow rate 0.1 mL/mL, and the column was washed successively with distilled water and three cycles of alternating pH. Each cycle consisted of a wash with 0.1 M acetic acid/sodium acetate, at pH 4.0, containing 0.5 M NaCl, followed by a wash with 0.1 M Tris-HCl, at pH 8.0, containing 0.5 M NaCl. Finally, the column was washed with distilled water and equilibrated with binding buffer (PBS with 1 M NaCl, pH 7.4). The amount of matrix-coupled peptide was estimated spectrophotometrically by comparing absorbances of peptide solutions at 280 nm recorded before and after the coupling procedure.

One milliliter of PBS spiked with human IgG and BSA in a 1:1 mass ratio (2 mg each) was injected onto the affinity column at a flow rate of 0.1 mL/min. When the unbound material passed through the column, the flow rate was increased to 0.3 mL/min for the remainder of the run. The column was extensively washed with binding buffer, and the bound material was eluted with 50 mM Gly·HCl, at pH 2.5. Eluted fractions were neutralized with 1 M Tris·HCl, at pH 9, immediately after collection. Collected 0.2 mL chromatographic fractions were analyzed by SDS-PAGE.

To estimate the dynamic binding capacity of the affinity column, 1 mL aliquots of human IgG at defined concentrations (200−3000 μg/mL; Figure S6) in binding buffer were injected into the chromatograph, bypassing the column, and resulting peaks were integrated to construct a standard curve by plotting the peak areas (AUC) against the amount of injected IgGs. Finally, 5 mg of human IgG was injected onto the column in 1 mL of binding buffer, and after extensive washing, bound material was released with the elution buffer. The amount of eluted IgG was calculated from the elution peak areas using the standard curve.

Purification of IgG from spiked growth medium (2.5 mg IgG/mL complete DMEM) and human serum diluted 1:1 with PBS containing 2 M NaCl was performed essentially as described for IgG/BSA-spiked PBS.

Statistical Analyses. In replicate experiments, results are reported as arithmetic mean ± standard deviation.

DOI: 10.1021/acs.bioconjchem.8b00395
Bioconjugate Chem. 2018, 29, 2763−2775

■ ASSOCIATED CONTENT

Supporting Information

The Supporting Information is available free of charge on the ACS Publications website at DOI: 10.1021/acs.bioconjchem.8b00395.

Demonstration of phage display affinity selection progression for panning PhD-12 library; functional screening data for Fc-binding phage clones; detailed procedures of M13KBE phage display vector preparation and molecular cloning procedures to construct divalent phage; surface plasmon resonance sensorgrams of hFc:min19Fc interaction; list of all oligonucleotides used in this study; standard curve for estimation of dynamic binding capacity of affinity column; performance of affinity column in purification of IgG from spiked complete DMEM and crude human serum (PDF)

■ AUTHOR INFORMATION

Corresponding Author

*Address: University of Ljubljana, Faculty of Pharmacy, Department for Pharmaceutical Biology, Aškerčeva 7, SI-1000 Ljubljana, Slovenia. Phone: +386 1 4769 570. Fax: +386 1 4258 031. E-mail: tomaz.bratkovic@ffa.uni-lj.si.

ORCID

Tomaž Bratkovič: 0000-0001-8367-5465

Notes

The authors declare no competing financial interest.

■ ACKNOWLEDGMENTS

We are grateful to Monika Sonc from the Institute of Oncology, Ljubljana, and prof. Peter Černelč and prof. Ivan Ferkolj from the University Medical Center, Ljubljana, for providing leftover therapeutic antibodies from multidose vials. This work was supported by the Slovenian Research Agency (program P4-0127).

■ ABBREVIATIONS

AUC, area under curve; (b-)hFc, (biotinylated) human Fc fragment; BSA, bovine serum albumin; DBC, dynamic binding capacity; ELISA, enzyme-linked immunosorbent assay; FITC, fluorescein isothiocyanate; FLISA, fluorescence-linked immunosorbent assay; HRP, horseradish peroxidase; HSA, human serum albumin; MST, microscale thermophoresis; PBS, phosphate buffered saline; PEG, polyethylene glycol; SA, streptavidin; SpA, staphylococcal protein A; SPR, surface plasmon resonance

■ REFERENCES

(1) Elgundi, Z., Reslan, M., Cruz, E., Sifniotis, V., and Kayser, V. (2017) The state-of-play and future of antibody therapeutics. *Adv. Drug Delivery Rev. 122*, 2−19.

(2) Shukla, A. A., Wolfe, L. S., Mostafa, S. S., and Norman, C. (2017) Evolving trends in mAb production processes. *Bioeng Transl Med. 2* (1), 58−69.

(3) Kelley, B. (2009) Industrialization of mAb production technology: the bioprocessing industry at a crossroads. *MAbs 1* (5), 443−52.

(4) Gronemeyer, P., Ditz, R., and Strube, J. (2014) Trends in upstream and downstream process development for antibody manufacturing. *Bioengineering 1* (4), 188−212.

(5) Singh, N., and Herzer, S. (2017) Downstream Processing technologies/capturing and final purification: opportunities for innovation, change, and improvement. A review of downstream processing developments in protein purification. *Adv. Biochem. Eng./Biotechnol.*, DOI: 10.1007/10_2017_12.

(6) Chon, J. H., and Zarbis-Papastoitsis, G. (2011) Advances in the production and downstream processing of antibodies. *New Biotechnol. 28* (5), 458−63.

(7) Bolton, G. R., and Mehta, K. K. (2016) The role of more than 40 years of improvement in protein A chromatography in the growth of the therapeutic antibody industry. *Biotechnol. Prog. 32* (5), 1193−1202.

(8) Hober, S., Nord, K., and Linhult, M. (2007) Protein A chromatography for antibody purification. *J. Chromatogr. B: Anal. Technol. Biomed. Life Sci. 848* (1), 40−7.

(9) Shukla, A. A., Hubbard, B., Tressel, T., Guhan, S., and Low, D. (2007) Downstream processing of monoclonal antibodies–application of platform approaches. *J. Chromatogr. B: Anal. Technol. Biomed. Life Sci. 848* (1), 28−39.

(10) Hahn, R., Shimahara, K., Steindl, F., and Jungbauer, A. (2006) Comparison of protein A affinity sorbents III. Life time study. *J. Chromatogr A 1102* (1−2), 224−31.

(11) Kruljec, N., and Bratkovič, T. (2017) Alternative Affinity Ligands for Immunoglobulins. *Bioconjugate Chem. 28* (8), 2009−2030.

(12) Verdoliva, A., Pannone, F., Rossi, M., Catello, S., and Manfredi, V. (2002) Affinity purification of polyclonal antibodies using a new all-D synthetic peptide ligand: comparison with protein A and protein G. *J. Immunol. Methods 271* (1−2), 77−88.

(13) Yang, H., Gurgel, P. V., Williams, D. K., Jr., Bobay, B. G., Cavanagh, J., Muddiman, D. C., and Carbonell, R. G. (2010) Binding site on human immunoglobulin G for the affinity ligand HWRGWV. *J. Mol. Recognit. 23* (3), 271−82.

(14) Yang, H., Gurgel, P. V., and Carbonell, R. G. (2009) Purification of human immunoglobulin G via Fc-specific small peptide ligand affinity chromatography. *J. Chromatogr A 1216* (6), 910−8.

(15) Yang, H., Gurgel, P. V., and Carbonell, R. G. (2005) Hexamer peptide affinity resins that bind the Fc region of human immunoglobulin G. *J. Pept. Res. 66*, 120−137.

(16) Zhao, W. W., Liu, F. F., Shi, Q. H., Dong, X. Y., and Sun, Y. (2014) Biomimetic design of affinity peptide ligands for human IgG based on protein A-IgG complex. *Biochem. Eng. J. 88*, 1−11.

(17) Sugita, T., Katayama, M., Okochi, M., Kato, R., Ichihara, T., and Honda, H. (2013) Screening of peptide ligands that bind to the Fc region of IgG using peptide array and its application to affinity purification of antibody. *Biochem. Eng. J. 79*, 33−40.

(18) Dias, R. L., Fasan, R., Moehle, K., Renard, A., Obrecht, D., and Robinson, J. A. (2006) Protein ligand design: from phage display to synthetic protein epitope mimetics in human antibody Fc-binding peptidomimetics. *J. Am. Chem. Soc. 128* (8), 2726−32.

(19) Gong, Y., Zhang, L., Li, J., Feng, S., and Deng, H. (2016) Development of the Double Cyclic Peptide Ligand for Antibody Purification and Protein Detection. *Bioconjugate Chem. 27* (7), 1569−73.

(20) Menegatti, S., Hussain, M., Naik, A. D., Carbonell, R. G., and Rao, B. M. (2013) mRNA display selection and solid-phase synthesis of Fc-binding cyclic peptide affinity ligands. *Biotechnol. Bioeng. 110* (3), 857−70.

(21) D'Agostino, B., Bellofiore, P., De Martino, T., Punzo, C., Rivieccio, V., and Verdoliva, A. (2008) Affinity purification of IgG monoclonal antibodies using the D-PAM synthetic ligand: chromatographic comparison with protein A and thermodynamic investigation of the D-PAM/IgG interaction. *J. Immunol. Methods 333* (1−2), 126−38.

(22) Dinon, F., Salvalaglio, M., Gallotta, A., Beneduce, L., Pengo, P., Cavallotti, C., and Fassina, G. (2011) Structural refinement of protein A mimetic peptide. *J. Mol. Recognit. 24* (6), 1087−94.

(23) Krook, M., Mosbach, K., and Ramstrom, O. (1998) Novel peptides binding to the Fc-portion of immunoglobulins obtained from a combinatorial phage display peptide library. *J. Immunol. Methods 221* (1−2), 151−7.
(24) DeLano, W. L., Ultsch, M. H., de Vos, A. M., and Wells, J. A. (2000) Convergent solutions to binding at a protein-protein interface. *Science 287* (5456), 1279−1283.
(25) Ehrlich, G. K., and Bailon, P. (2001) Identification of model peptides as affinity ligands for the purification of humanized monoclonal antibodies by means of phage display. *J. Biochem. Biophys. Methods 49* (1), 443−454.
(26) Ehrlich, G. K., and Bailon, P. (1998) Identification of peptides that bind to the constant region of a humanized IgG1 monoclonal antibody using phage display. *J. Mol. Recognit. 11* (1−6), 121−5.
(27) Deisenhofer, J. (1981) Crystallographic refinement and atomic models of a human Fc fragment and its complex with fragment B of protein A from Staphylococcus aureus at 2.9- and 2.8-A resolution. *Biochemistry 20* (9), 2361−70.
(28) Kokoszka, M. E., and Kay, B. K. (2015) Mapping Protein-Protein Interactions with Phage-Displayed Combinatorial Peptide Libraries and Alanine Scanning. *Methods Mol. Biol. 1248*, 173−188.
(29) Karlsson, R., Katsamba, P. S., Nordin, H., Pol, E., and Myszka, D. G. (2006) Analyzing a kinetic titration series using affinity biosensors. *Anal. Biochem. 349* (1), 136−47.
(30) Gradišar, H., and Jerala, R. (2011) De novo design of orthogonal peptide pairs forming parallel coiled-coil heterodimers. *J. Pept. Sci. 17* (2), 100−6.
(31) Moiani, D., Salvalaglio, M., Cavallotti, C., Bujacz, A., Redzynia, I., Bujacz, G., Dinon, F., Pengo, P., and Fassina, G. (2009) Structural characterization of a Protein A mimetic peptide dendrimer bound to human IgG. *J. Phys. Chem. B 113* (50), 16268−75.
(32) Jerabek-Willemsen, M., Wienken, C. J., Braun, D., Baaske, P., and Duhr, S. (2011) Molecular interaction studies using microscale thermophoresis. *Assay Drug Dev. Technol. 9* (4), 342−53.
(33) Naik, A. D., Menegatti, S., Gurgel, P. V., and Carbonell, R. G. (2011) Performance of hexamer peptide ligands for affinity purification of immunoglobulin G from commercial cell culture media. *J. Chromatogr A 1218* (13), 1691−700.
(34) Zhao, W. W., Shi, Q. H., and Sun, Y. (2014) FYWHCLDE-based affinity chromatography of IgG: effect of ligand density and purifications of human IgG and monoclonal antibody. *J. Chromatogr A 1355*, 107−14.
(35) Smith, G. P., and Petrenko, V. A. (1997) Phage display. *Chem. Rev. 97* (2), 391−410.
(36) Day, L. A., and Wiseman, R. R. (1978) *A Comparison of DNA Packaging in the Virions of fd, Xf, and Pf1*, Vol. *08*, pp 605−625, Cold Spring Harbor, New York.
(37) Bratkovič, T., Lunder, M., Popovič, T., Kreft, S., Turk, B., Štrukelj, B., and Urleb, U. (2005) Affinity selection to papain yields potent peptide inhibitors of cathepsins L, B, H, and K. *Biochem. Biophys. Res. Commun. 332* (3), 897−903.

DOI: 10.1021/acs.bioconjchem.8b00395
Bioconjugate Chem. 2018, 29, 2763−2775